Research Article

Thanh Q. C. Nguyen, Huy B. Tran, Nghia K. Nguyen, Nhut M. Nguyen, and Giao H. Dang*

Removal efficiency of dibenzofuran using CuZn-zeolitic imidazole frameworks as a catalyst and adsorbent

https://doi.org/10.1515/gps-2022-8112
received September 16, 2022; accepted December 13, 2022

Abstract: Dioxins/furans are classified as highly toxic chemicals that seriously affect human health. To remove dioxin residues from contaminated water, CuZn-ZIFs, a material from bimetallic zeolitic imidazolate frameworks (ZIFs) has been synthesized and explored its efficacy treatment with dibenzofuran (DBF). The pristine structure of CuZn-ZIFs was confirmed using powder X-ray diffraction, Fourier-transform infrared, thermogravimetric analysis, energy-dispersive X-ray, Brunauer–Emmett–Teller, and scanning electron microscopy. CuZn-ZIFs exhibited its role as a heterogeneous catalyst promoting H_2O_2 oxidation and as an adsorbent in DBF treatment. Herein, at room temperature, more than 86% of DBF adsorbed and 90% of DBF degraded in the presence of H_2O_2 with 10 mg catalyst dosage, 30 ppm of DBF within 40 and 60 min, respectively. Remarkably, the CuZn-ZIFs' reusability of each process showed a high efficacy removal with over 80% after five cycles. Therefore, CuZn-ZIFs synthesized could be a prospective candidate for the indirect or direct degradation of dioxins/DBF derivatives from contaminated water.

Keywords: adsorption, bimetallic, catalyst, dibenzofuran, zeolitic imidazolate framework

*** Corresponding author: Giao H. Dang,** Faculty of Chemical Engineering, College of Engineering Technology, Can Tho University, Campus II, 3/2 Street, Ninh Kieu District, Can Tho City, Vietnam, e-mail: dhgiao@ctu.edu.vn,
tel: +84-292 3834267, fax: +84-292 3831151
Thanh Q. C. Nguyen: Department of Chemistry, College of Natural Sciences, Can Tho University, Campus II, 3/2 Street, Ninh Kieu District, Can Tho City, Vietnam
Huy B. Tran, Nhut M. Nguyen: Faculty of Chemical Engineering, College of Engineering Technology, Can Tho University, Campus II, 3/2 Street, Ninh Kieu District, Can Tho City, Vietnam
Nghia K. Nguyen: Faculty of Soil Science, College of Agriculture, Can Tho University, Campus II, 3/2 Street, Ninh Kieu District, Can Tho City, Vietnam

1 Introduction

Dioxins (polychlorinated dibenzo-*p*-dioxins/dibenzofurans, PCDD/Fs) are a group of highly toxic chemical compounds and belong to the classification of unintentionally produced persistent organic pollutants (UP-POPs) [1]. Dioxins are considered as by-products of human industrial processes, including chemical production, the paper industry, and the manufacturing of herbicides [2]. Besides, dioxins and furans were found in chemical combustion, forest fires, and the addition of natural events such as volcanic eruptions. Historically, dioxins and furans were used as "orange agent-herbicides" in the Vietnam War of 1957–1971 to wipe out food crops, causing the starvation of the Vietnamese soldiers and to win quickly [3]. Seriously, exposure to dioxin via different routes negatively affects human health and the environment, and is classified into Group I carcinogens and mutagens [4]. The accumulation of dioxins in adipose tissues is related to reproductive system disorders, immune system damage, and adverse effects on hormonal pathways. Thus, dioxins are known as the "poisons of the century" and is one of the world's most toxic compounds [3]. According to previous reports, these poisonous pollutants are a historical problem in the environment, including soil, water, and air, mainly due to their slow decomposition, which ranges from decades to centuries, and bioaccumulative behavior [5–9]. Therefore, the effort to eliminate and degrade these recalcitrant pollutants still remains a challenge, particularly in water (surface water or groundwater).

Recently, the detoxification and degradation processes, including thermal processes, photodegradation, chemical interventions, and dechlorination methods aided by metal catalysts, have been evaluated as a potential solution to free the environment from harmful toxics [10]. Significantly, advanced oxidation processes (AOPs) enhanced the bio-treatability and the mineralization of organic compounds obtaining remarkable results. The Fenton oxidation technology, based on a typical reaction of AOPs, has been proposed as an attractive candidate for

the removal of persistent organic pollutants in water and soil at large scales, such as fertilizers, dyes, aromatic compounds, and their derivatives [11]. This technology is based on activating an oxidant agent to generate strong oxidant-free radicals using metal or metal oxides. Nevertheless, due to the non-selective properties of reactive free radicals, they are able to destroy a wide range of organic substrates [12]. To overcome these drawbacks, the Fenton-like heterogeneous catalyst has been researched with advantages such as high efficiency, minimum leaching, recyclability, environmental friendliness, and stability over long application periods [13]. Moreover, the requirements of its characters must be a well-defined porous nature with high stabilities and a large surface area [14]. Thus, the catalysts composed of transition metals are ideally suited to exhibit multiple oxidation states suitable for the redox cycle [15].

Zeolitic imidazole frameworks (ZIFs), as a subfamily of microporous metal crystalline organic frameworks, are constructed via coordination bonding between metal ions (zinc or cobalt ions) and imidazolate-type linkers, and have become a potential candidate for fabricating new materials [16]. Interestingly, ZIFs have expanded their applications in various fields such as catalysis, medical, chemical separation, and adsorption due to their structural diversity and special characterization, such as high surface area, high crystallinity, large pore volume, and tunable porosity [17]. In detail, the zinc-based ZIF (ZIF-8) has been reported as a heterogeneous catalyst for oxidation of limonene or Michael reaction, adsorption for methyl blue/methyl orange in the dye, rhodamine B dye degradation, adsorption of gas using dye encapsulated hierarchical porous ZIF-8, and catalyst of hydrogen gas released from hydrides using a hierarchical porous zeolitic imidazolate framework (HPZIF-8) [18–24]. Notably, the magnetic Fe_3O_4/ZIF-8 composites or a porous solid base catalyst (ZIF-90-Gua) have been synthesized with expected catalytic performance and were easily reused to improve the biodiesel production process [25,26]. The typical single-meta ZIFs as zinc exhibit many outstanding properties due to the large microporous surfaces and a high degree of nitrogen doping but are also limited by low degree graphitization. Therefore, the heterogeneous catalyst was prepared by mixing two different metal ions having identical ionic radii within the framework to enhance the activity. Bimetallic ZIF synthesis of bimetallic ZIFs became one of the important strategies in catalyst development due to the synthetic flexibility in incorporating two different metal ions without affecting the framework structure [20]. The relatively superior performance of these materials has been demonstrated in many previous studies [16,27,28]. Furthermore, iron-dopped (FeZIF-8) was conducted as a photocatalyst for rhodamine B dye degradation [19]. Adding cobalt into ZIF-8 as bimetallic Co/Zn-ZIF-8 enhanced its efficacy in promoting H_2O_2 oxidation for the destruction of organic dyes [29]. Among the AOPs treatment methods of PCDD/Fs, Fenton-based processes are effective and simple wastewater treatments for the removal of PCDD/Fs since they can degrade many organic compounds. Several studies on Fenton oxidation processes for the treatment of polluted waters have been reported in the literature [30–35]. However, most of those studies used Fe^{2+} as a catalyst and combined it with other AOP methods to degrade PCDD/Fs in aqueous solutions. As a result, the performance of the removal of PCDD/Fs from wastewater is hindered by the lack of experimental studies using various materials, which are a key factor in the whole process. According to the literature review and the previous studies, it can be observed that ZIF materials are advantageous for the decomposition of organic compounds due to their adsorption and catalytic properties. To this end, using bimetallic ZIFs as the Fenton-like heterogeneous catalyst is a promising solution for UP-POPs removal in water.

In this work, the bimetallic CuZn-ZIFs are synthesized with full characterization presented and selected for dibenzofuran (DBF) treatment in contaminated water under simulated laboratory conditions. The role of CuZn-ZIFs for direct/indirect DBF removal based on its properties as adsorption and catalytic activity is investigated as well. Regarding the optimal conditions for each treatment process, the effect of various parameters, i.e., catalyst dosage, time, temperature, and initial DBF concentration on the DBF removal efficacy by CuZn-ZIFs with or without the presence of H_2O_2 has been proposed. Finally, the efficiency of material reusability is also determined. Thus, this study proposes a novel material as well as its application, CuZn-ZIFs, to efficiently eliminate the persistent organic pollutants in an aqueous solution, particularly DBF derivatives.

2 Materials and methods

2.1 Materials

Zinc nitrate hexahydrate ($Zn(NO_3)_2{\cdot}6H_2O$) and copper (II) nitrate trihydrate ($Cu(NO_3)_2{\cdot}3H_2O$) were purchased from Sigma-Aldrich (purity 99%). 2-Methylimidazole (2-MIm, $C_4H_6N_2$) was purchased from Acros (purity 99%). Methanol (CH_3OH), DBF ($C_{12}H_8O$), and hydrogen peroxide (H_2O_2) were

purchased from Xilong Chemical Co., Ltd, China (purity 99%).

2.2 Synthesis of CuZn-ZIFs

CuZn-ZIFs (Cu/ZIF-8) were synthesized following the previous report with slight modifications [36]. Briefly, the molar ratio of $Cu(NO_3)_2{\cdot}3H_2O$ and $Zn(NO_3)_2{\cdot}6H_2O$ was fixed to 1:3. Then, the mixture mentioned above and 2-MIm was separately prepared by dissolving in 20 mL methanol. Afterward, the homogenous mixture was gradually dropped into the 2-MIm solution under magnetic stirring for 30 min and sonicated for 15 min at 60°C to ensure that the mixture formed a pale pink crystallization. After that, the crystals obtained were kept at room temperature for 24 h. The precipitates were then collected by centrifugation at 6,000 rpm within 15 min. The pale pink solid was immersed in 10 mL of methanol for 2 h and then centrifuged to remove the solvent before adding the same amount of methanol for the next step. The process was repeated several times to discard impurities from the materials completely. Finally, CuZn-ZIFs were obtained by drying at 60°C for 24 h.

2.3 Characterization of CuZn-ZIFs

The CuZn-ZIFs characteristic was analyzed by using several techniques, including powder X-ray diffraction (PXRD, CuKα [$\lambda = 1.5405$ Å] radiation source, D8 Advance – Brucker powder diffraction meter); the internal morphologies and structural features were observed by the scanning electron microscopy (SEM, Hitachi S4800). The surface area of CuZn-ZIFs was examined by the Brunauer–Emmett–Teller (BET) method. The Fourier-transform infrared spectroscopy (FT-IR) was recorded to determine the samples' specific links. Besides, thermogravimetric analysis (TGA) was performed on Setaram Labsys Evo with a heating rate of $10°C{\cdot}min^{-1}$ in the air atmosphere.

2.4 Degradation experiment

DBF treatment by CuZn-ZIFs was conducted to investigate the various affecting factors, including DBF concentration, concentration of H_2O_2, the amount of materials, temperature, and reaction time. In detail, a defined amount of CuZn-ZIFs was evenly dispersed into 10 mL of DBF at various concentrations (0–60 ppm) with the presence or absence of H_2O_2 (0–0.025 $mol{\cdot}L^{-1}$). The kinetics of this reaction was investigated at different time intervals (20–100 min) and temperatures (from room temperature to 60°C). Then, the entire solution after filtration was collected to measure the absorbance. The efficacy of the DBF processing was analyzed at 280 nm using a V-730 UV-Vis spectrophotometer (Jasco, Tokyo, Japan) and calculated as per the equation in the previous report [13].

2.5 Reusability of CuZn-ZIFs

The process of recovering and evaluating the reusability of CuZn-ZIFs was carried out under the optimal conditions of DBF degradation. Subsequently, the material was collected by centrifugation and washed several times. Dried at 60°C for 24 h after washing, the regenerated CuZn-ZIFs were re-analyzed to assess their structural stability by PXRD and FT-IR spectroscopy.

3 Results and discussion

3.1 Structure and morphological characterization of CuZn-ZIFs

CuZn-ZIFs, as formed bimetallic Cu/Zn ZIFs, had been successfully synthesized using a heating method supported by ultrasonic waves based on the research by Zhang and Liu [36]. XRD analysis was used to compare the crystal structure of CuZn-ZIFs and ZIF-8. As shown in Figure 1a, XRD patterns appeared with the main diffraction signals present at 7.3°, 10.3°, 12.7°, 14.7°, 16.4°, 18°, 24.6°, and 26.7° corresponding to the sides (011), (002), (112), (022), (013), (222), (144), and (233), respectively, and were identified in comparison with ZIF-8. This result proved that the material has a multifaceted structure with high sharpness signal as evidence of obtaining crystallization material. Additionally, the similarity of characteristic peaks indicated that adding Cu^{2+} did not affect crystal formation, and the material structure was preserved due to the similar ionic size between Cu^{2+} and Zn^{2+} [20]. Thus, this pattern demonstrated that CuZn-ZIFs were

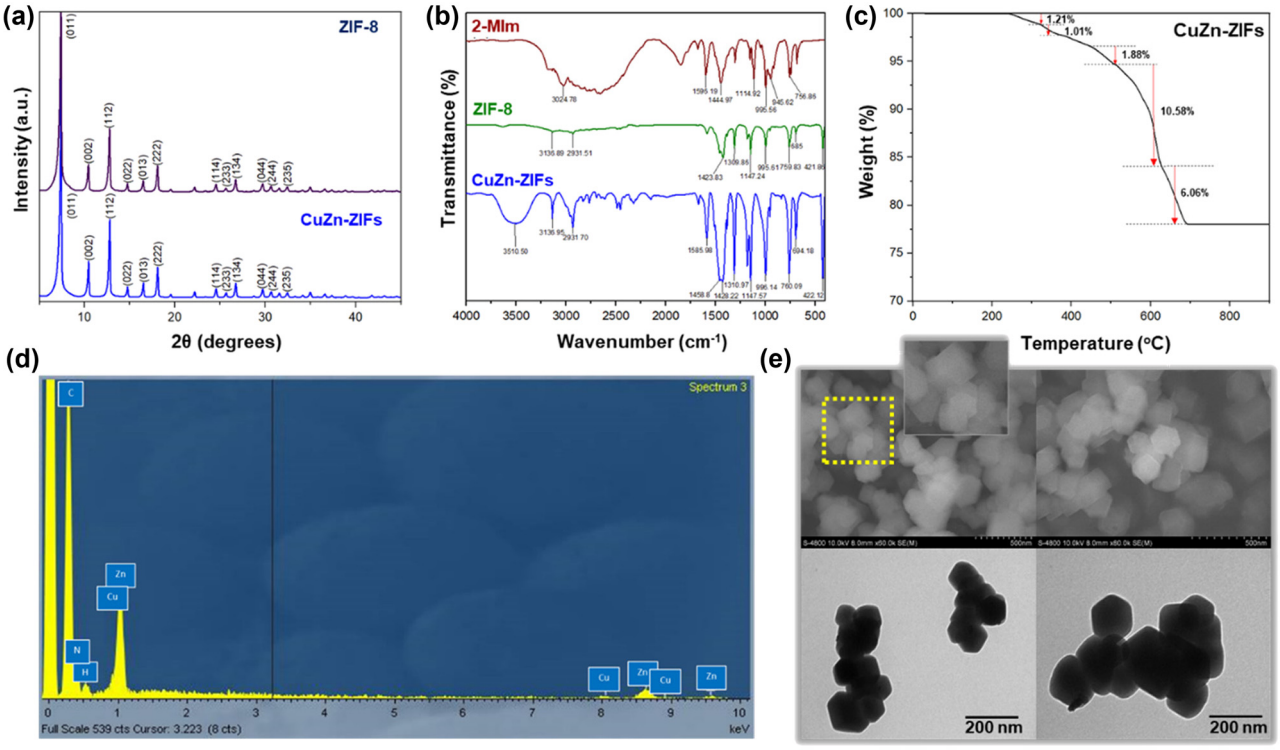

Figure 1: (a) X-ray diffraction patterns of ZIF-8 and CuZn-ZIFs, (b) FT-IR patterns of ZIF-8 and CuZn-ZIFs, (c) TGA curve of CuZn-ZIFs, (d) EDX spectrum of CuZn-ZIFs, and (e) SEM and TEM images of CuZn-ZIFs.

successfully synthesized as structural homologs of ZIF-8 [37].

The presence of distinct functional groups via chemical bonds was determined by FI-IR spectroscopy. As illustrated in Figure 1b, the values of signals ranging from 600 to 1,600 cm^{-1} were due to the characteristic stretching and bending of 2-MIm. Remarkably, a sharp peak at 421.86 cm^{-1} (ZIF-8 pattern) or 422.12 cm^{-1} attributing to Zn–N stretching mode and the range of 550–620 cm^{-1} (Figure A8 in Appendix) was assigned for Cu–N bonding vibration as mentioned in the previous report [20,38]. Moreover, the absence of broadband from 2,200 to 3,200 cm^{-1} and a peak at 1,850 cm^{-1} concluded that CuZn-ZIFs and ZIF-8 were formed completely [24,37]. Overall, the position of peaks is consistent with the previously published report [39]. As expected, the result confirmed the successful synthesis of CuZn-ZIFs with the structure integrity maintained.

The morphology and structure of CuZn-ZIFs were determined using SEM and transmission electron microscopy (TEM). These images clearly showed that the sample dispersed and has a rhombus-shaped dodecahedron structure with an average diameter of around 200 nm (Figure 1e). Therefore, the framework structure and crystal morphology were not altered during the doping of Cu^{2+}. It is noteworthy to mention that regardless of the doping ratio between Cu^{2+} and Zn^{2+} in the framework, the images showed quite small and single-dispersion well-defined truncated rhombohedral dodecahedron structure, which is a typical ZIF-8 morphology [40]. Additionally, the BET analysis of CuZn-ZIFs showed that the specific surface area was slightly lower than ZIF-8 at 1,004.41 $m^2 \cdot g^{-1}$ (Figure A6), consistent with the previous reports [40–42]. Furthermore, the energy-dispersive X-ray (EDX) spectrums verified the presence of four main elements in bimetal CuZn-ZIFs, including C, N, Zn, and Cu, as shown in Figure 1d [38]. TGA of CuZn-ZIFs showed that the weight decreases gradually as a descending curve from 250°C to 400°C, which could be explained possibly due to the escape of impurities and gas molecules (Figure 1c). In addition, the weight depletion of CuZn-ZIFs happened between 500°C and 700°C via the decomposition of the ligand 2-MIm in the framework of CuZn-ZIFs, consistent with the previous studies [36,43]. The high thermal stability of this synthesized material was noticeable due to the presence of monometallic copper in ZIF-8 [38]. Finally, CuZn-ZIFs were successfully synthesized with similar characterization of ZIF-8 for further experiments.

3.2 Role of CuZn-ZIFs activity on DBF treatment

DBF toxicity residue treatment in contaminated water using CuZn-ZIFs was evaluated based on its properties, including adsorption and catalysis. In most of the studies devoted to wastewater or polluted water, the toxicity assessment is conducted to confirm no toxic effect for particular species. However, a previous report noted that the toxicity of H_2O_2 related to the treatment might affect aquatic organisms and plants [44]. Thus, this study comprehensively evaluated this material's role in indirect and direct treatment. The proposed DBF indirect treatment was based on the adsorption properties of material similar to a previous study [18,45]. In contrast, following the Fenton-like reaction mechanism, adding a catalyst to enhance H_2O_2 decomposition into free radicals is considered a potential solution for DBF direct treatment [29]. Nevertheless, to conclude that the sole presence of metal in the nodes contributed to or non-contributed to H_2O_2 catalytic decomposition by either radical or redox mechanism requires further study. In a simple way, according to previous studies, the proposal of H_2O_2 decomposition on a solid surface was a spontaneous process from room temperature up to 286°C, as follows: (1) the radical mechanism, as a Fenton-like reaction, is based on the complexation between catalyst surface and H_2O_2 following a series of reactions that cause H_2O_2 decomposition to release $^{\bullet}OH$ and $HO_2^{\bullet}$ [11,29,46]; (2) the redox mechanism following the Haber–Weiss mechanism to release $^{\bullet}OH$ and $HO_2^{\bullet}$ [11]. For the present work, the role CuZn-ZIFs activity on DBF treatment during adsorption and catalyst was influenced by various factors, including DBF concentration, H_2O_2 concentration, catalyst dosage, temperature, and reaction time. Therefore, the factors were investigated to optimize the conditions for the DBF treatment process.

DBF concentration is a critical factor to investigate for applying the material. Dioxin or DBF derivatives appeared at low doses in contaminated water [47]. Hence, DBF concentration in the experiment needs to be considered to achieve the optimal effect. In order to investigate the DBF concentration, the other factors were randomly fixed with specific parameter conditions. As shown in Figure 2, the DBF removal efficiency of adsorption and catalyzing was constant up to 30 ppm, reaching 87% and 93%, respectively. Nevertheless, a high concentration of DBF from 40 to 60 ppm showed a steady decrease in the treatment efficiency. It can be explained that the high concentration of DBF required more doses of material to adsorb

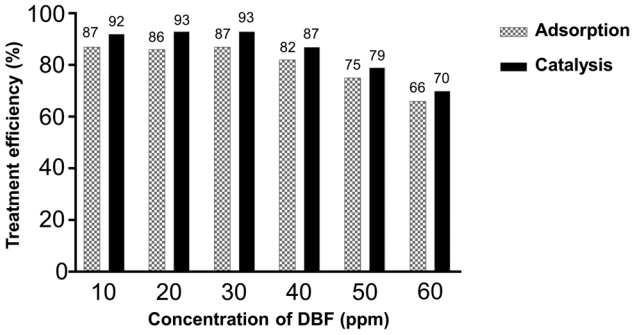

Figure 2: Effect of DBF concentration on the degradation efficiency. Catalysis: [H_2O_2] = 10 mM; catalyst dosage = 10 mg, room temperature, time = 60 min. Absorption: adsorbent dosage = 10 mg, room temperature, time = 60 min.

comprehensively and more free radicals to degrade. Thus, 30 ppm was selected as the optimal DBF initial concentration for further experiments.

The role of CuZn-ZIFs catalyst is based on H_2O_2 activation to generate $^{\bullet}OH$ free radicals following the above-proposed mechanism. Thus, the effect of H_2O_2 concentration on the DBF degradation efficiency was evaluated from 0 to 25 mM, and other parameters were fixed. The removal efficiency of DBF was increased to 15 mM at the highest value of 94%. Then the degradation efficiency of DBF was decreased and stabilized at 91% and 92% over the concentration range from 20 to 25 mM (Figure 3). It can be explained that a tremendous amount of free radicals released are higher than required for DBF degradation. Consequently, these radicals attack themselves to generate perhydroxyl radical that is less oxidative than hydroxy resulting in reduced yield [46]. Additionally, DBF adsorption efficiency was at a high value of 84% in the absence of H_2O_2 (0 mM). The result suggests that

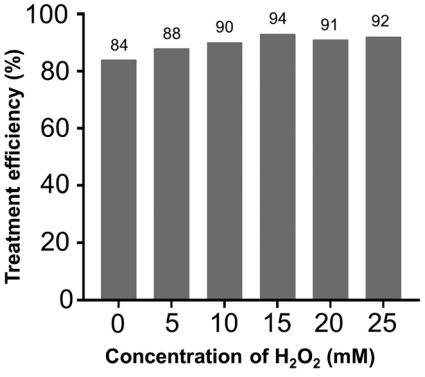

Figure 3: Effect of H_2O_2 concentration on the DBF degradation efficiency. [DBF] = 30 ppm, catalyst dosage = 10 mg, room temperature, time = 60 min.

DBF treatment efficiency was increased by about 10% between adsorption and catalyst. Therefore, additional H_2O_2 significantly increased DBF processing capacity. CuZn-ZIFs may be promising for the direct or indirect treatment of DBF in contaminated water. Finally, the optimal H_2O_2 concentration was chosen at 15 mM for further experiments.

The CuZn-ZIFs dosage plays a critical role in the direct or indirect treatment of DBF through adsorption into the material's surface and H_2O_2 catalytic to generate $^{\bullet}OH$ free radicals. To determine the role of CuZn-ZIFs in the DBF treatment, a range of material dosages from 0 to 15 mg were investigated with the above-fixed parameters.

Generally, the yield of DBF treatment significantly increased with the increase of CuZn-ZIFs dosage. As seen in Figure 4, the treatment efficiency of DBF was at low level in the absence of CuZn-ZIFs. However, the treatment yield of DBF significantly increased from 72% to 85% for adsorption and 78% to 93% for catalyst since the addition of CuZn-ZIFs dosage from 5 up to 10 mg. Then the treatment reached a stable level at a material dosage of up to 15 mg. Hence, the highest yield could be achieved at 85% for adsorption and 93% for catalyst with 10 mg of CuZn-ZIFs. The result indicated that the presence of CuZn-ZIFs significantly increased the DBF removal efficiency by over 50% in comparison with only H_2O_2. Notably, the balance of adsorption or catalyst occurred, since the total active sites on the catalyst surface were limited by the uneven dispersion of material into the solution [48]. Thus, the adsorption or catalyst process cannot be increased when reaching equilibrium even with the increasing material dosage. Besides, as mentioned above, the reaction of these free radicals in the catalyst process was also a cause leading to the limitation of DBF removal efficiency. Conclusively, 10 mg of CuZn-ZIFs was selected for further experiments.

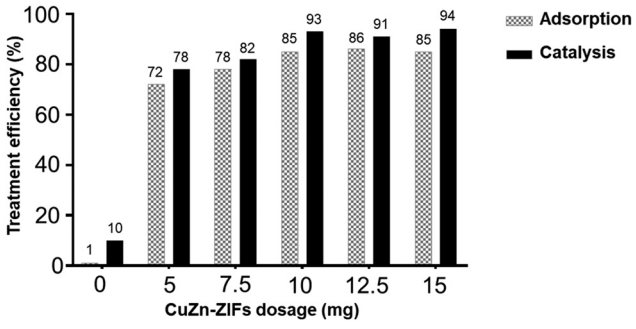

Figure 4: Effect of material dosage on the DBF removal efficiency. Catalysis: [DBF] = 30 ppm, $[H_2O_2]$ = 15 mM. Adsorption: [DBF] = 30 ppm, room temperature, time = 60 min.

An increase in temperature leads to a rise in the average kinetic energy of molecules. Thus, the changes in temperature factor directly affect the rate of reaction. As shown in Figure 5, the result indicated the difference in DBF treatment efficiency between adsorption and catalyst. In detail, the treatment efficiency of DBF in the adsorption process steadily decreased with the increase from room temperature to 60°C. In contrast, the degradation efficiency of DBF in CuZn-ZIFs catalyst was 93% at room temperature, and the yield slightly increased to 94% at 40°C and 50°C. The highest yield of DBF treatment was 96% at 60°C. However, the yield was not significantly different in the temperature investigated. Accordingly, the temperature increase did not affect the DBF degradation for the catalyst process. In order to be simple for further experiments, the room temperature was selected.

Regarding the treatment efficiency of DBF using CuZn-ZIFs, the time factor related to the reaction rate was investigated. A series of experiments were evaluated from 20 to 100 min, as shown in Figure 6. For the adsorption process, the stable efficiency of DBF treatment achieved 86% and 85% from 40 and 60 min periods, respectively. After that, the yield dropped to 76% when the time was continuously increased up to 100 min. On the contrary, the efficiency of DBF degradation was significantly increased from 20 to 80 min, reaching the highest value at 95% in 80 min. However, the yield shows no substantial difference from 60 to 100 min, at 93% and 94%, respectively. This result indicated the differences in the mechanism for adsorption and catalyst as described above. To this end, 40 min was an appropriate time for DBF adsorption, and 60 min was chosen for DBF degradation.

In summary, the optimal conditions for DBF treatment using CuZn-ZIFs were described, including 10 mg

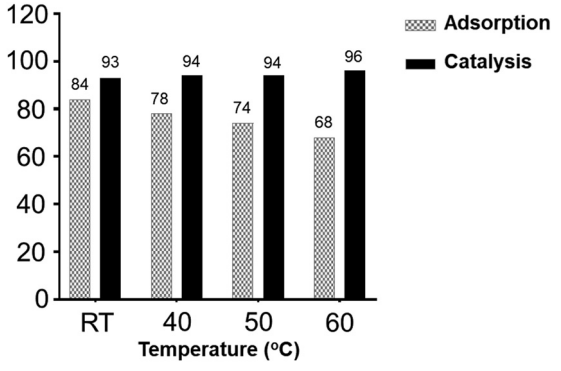

Figure 5: Effect of temperature on the DBF removal efficiency. Catalysis: [DBF] = 30 ppm, $[H_2O_2]$ = 15 mM, catalyst dosage = 10 mg, time = 60 min. Adsorption: [DBF] = 30 ppm, adsorbent dosage = 10 mg, time = 60 min.

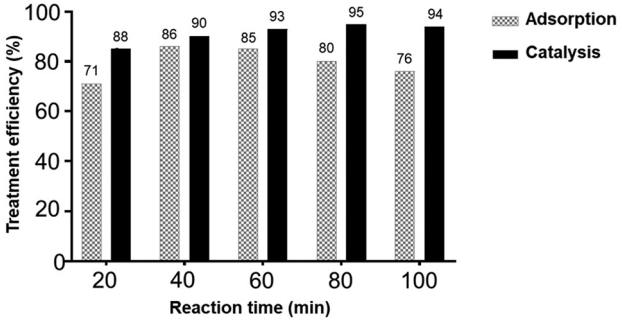

Figure 6: Effect of time on the DBF removal efficiency. Catalysis: [DBF] = 30 ppm, [H_2O_2] = 15 mM, catalyst dosage = 10 mg, room temperature. Adsorption: [DBF] = 30 ppm, adsorbent dosage = 10 mg, room temperature.

CuZn-ZIFs, 30 ppm DBF concentration at room temperature in 40 min for adsorption, and 60 min for catalyst with the presence of 15 mM H_2O_2. In a previous study on evaluating the efficiency of surface and groundwater treatment in water treatment plants in Japan, it was found that the ability to remove most of the dioxin congeners was 87%. However, the influence of extent chlorination led to an uncontrolled increase of 2,3,7,8-tetrachlorodibenzofuran [49]. These results indicated that a small amount of CuZn-ZIFs can remove DBF efficiently at ambient temperature. Hence, the material shows its potential for further application to treat various types of persistent organic pollutants in water.

To confirm the role of CuZn-ZIFs activity in DBF treatment, DBF residue after material recovery in the experiment above was conducted. The chemical stability of ZIFs is fundamentally dependent on the strength of their metal–ligand coordination bonds. However, their structure exhibits instability and is easily broken under humid acidic conditions [50]. Here, adding 2% HCl (*v*/*v*) in material recovery could disrupt their structure to release DBF residue. As shown in Figure 7a, the acidic condition did not affect the DBF absorbance peaks at 250 and 280 nm. Besides, the DBF residue appeared with low density compared to DBF alone for the catalyst process (Figure 7a and c). It can be explained that it could be due to the adsorption properties of CuZn-ZIFs remaining after catalyzing H_2O_2 to release free radicals. Another reason could be due to DBF contamination during the filtration process. Noteworthy, the essential adsorption of CuZn-ZIFs was clearly described due to the presence of DBF with sharpness peaks. These results illustrated the role of CuZn-ZIFs during direct (catalyst) or indirect (adsorption) DBF treatment.

3.3 The efficiency of DBF degradation using CuZn-ZIFs in comparison with other catalysts

The catalytic activity of CuZn-ZIFs in DBF degradation was compared to various homogeneous and heterogeneous catalysts under the above optimal conditions. Herein, the homogeneous catalysts were evaluated, including 2-MIm, ferric nitrate salt, copper nitrate salt, zinc nitrate salt, cobalt nitrate, and silver nitrate salt. Besides, activated carbon, silica gel, zeolite, bentonite, ZIF-8, and

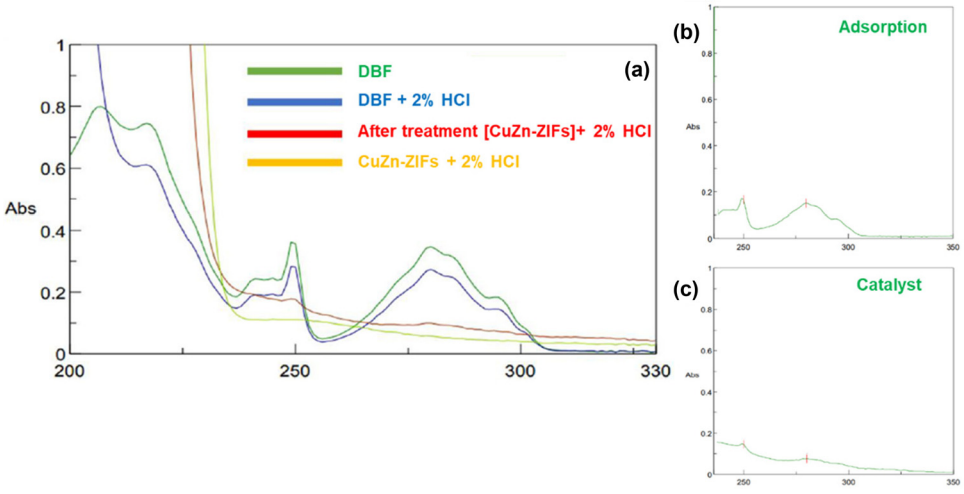

Figure 7: UV-Vis spectrum of DBF residue after CuZn-ZIFs recovery during adsorption and catalyst process. (a) Spectrum of DBF residue in CuZn-ZIFs before and after treatment compared with DBF alone and HCl addition for catalyst process, (b) DBF residue in the adsorption process, and (c) DBF residue in catalyst process.

ZIF-67 synthesized as a form of heterogeneous catalysts (Figures A1 and A2) were also investigated for the efficiency of DBF degradation compared with CuZn-ZIFs. The result indicated that the capacity removal of DBF using homogenous catalysts in the presence of H_2O_2 was less than 50%, whereas CuZn-ZIFs catalyst performed with the highest efficiency of DBF removal at 93% (Figure 8a). In detail, the catalytic of 2-Mim was lower than 10% and was attributed to the presence of H_2O_2 causing DBF degradation. Meanwhile, the degradation efficiency of DBF using cobalt and silver nitrate salt was at 44% and 40%, respectively. This indicated that the DBF removal was enhanced in the presence of metal ion and H_2O_2 according to the Fenton-like reaction [51–53]. Similarly, the DBF degradation efficiency using heterogeneous catalysts was still lower than 50%, except for ZIFs (Figure 8b). The result showed that the capacity of activated carbon, bentonite, and zeolite during DBF decomposition could be due to the adsorption of materials. Especially, activated carbon with porous surfaces possessed reducing properties to release active radicals. The decomposition proceeds were described as a classic Fenton-like reaction. However, pristine, unmodified carbon often performs poorly in catalytic wet peroxide oxidation, reducing DBF processing performance [54]. Besides, ZIF-8 and ZIF-67 catalysts in the presence of H_2O_2 were achieved at 80% and 85% for DBF degradation, respectively. However, the catalytic efficiency of CuZn-ZIFs was still higher than ZIF-67 and ZIF-8, by about 8–13%. This result indicated that bimetallic CuZn-ZIFs contained network nodes in the combination of both Zn^{2+} and Cu^{2+} ions to enhance H_2O_2 activation [55]. This point is further established that monometallic catalysts exhibit lower activity or selectivity than bimetallic catalysts. The bimetallic catalyst exhibited its desirable ability due to the synergistic effect between the two metal ions to trigger the reactants and reduce the energy barrier, especially in heterogeneous catalysis [56]. To this end, the yield of DBF degradation using CuZn-ZIFs catalyst in the presence of H_2O_2 was demonstrated in comparison with homogeneous and heterogeneous catalysts. These results offer great potential for direct DBF treatment in contaminated water.

3.4 The efficiency of CuZn-ZIFs reusability after DBF treatment

As the recyclability of a catalyst is an essential performance metric, the stability and reusability of CuZn-ZIFs after using DBF treatment directly and indirectly at optimal conditions were evaluated. Generally, no remarkable performance decay was observed after five consecutive cycles. As shown in Figure 9, the treatment efficiency was still maintained at over 80% for adsorption and over 90% for catalyst since the first cycle. In detail, the yield of DBF adsorption was stable at around 86% at three reuse cycles, then slightly decreased to 84% at the next cycle (Figure 9a). Moreover, the degradation efficiency slightly reduced from 92% to 90% after four reuse cycles since the first cycle. Additionally, the removal efficiency dropped down to 86% for the sixth cycle, illustrating CuZn-ZIFs' excellent reusability after treatments (Figure 9b). Obviously, the reason for high treatment efficiency might be due to the Cu-doped ZIF-8 metal-organic framework retaining its stable structure during processing. To confirm this hypothesis, the structural stability of CuZn-ZIFs was evaluated by PXRD and FT-IR analysis.

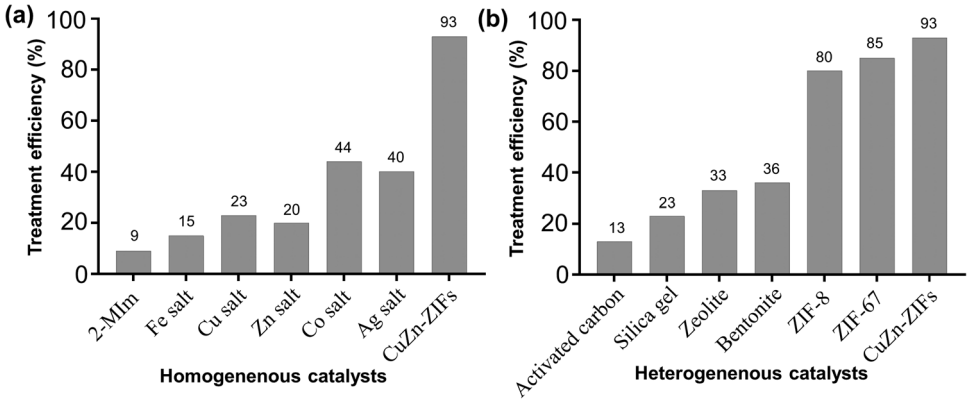

Figure 8: Efficiency of DBF degradation using CuZn-ZIFs in comparison with homogeneous catalyst and heterogeneous catalyst: (a) homogeneous catalysts and (b) heterogeneous catalysts. Catalysis: [DBF] = 30 ppm, [H_2O_2] = 15 mM, room temperature, catalyst dosage = 10 mg, time = 60 min.

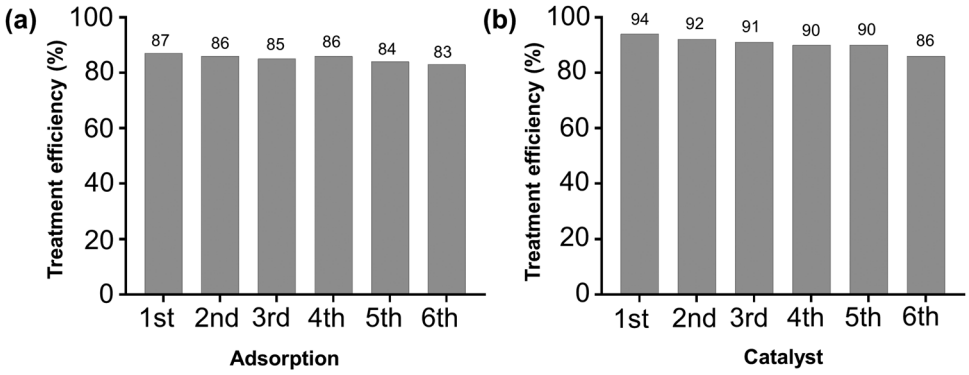

Figure 9: Efficiency of CuZn-ZIFs reusability after DBF treatment under optimal conditions. (a) adsorption, (b) catalyst.

FT-IR analysis showed those peaks of CuZn-ZIFs reused, in comparison with fresh material, still maintained the peaks at the characteristic positions, although there was a slight displacement, demonstrating the stable structure between metal ions and organic linkers. During adsorption and catalyst, the FT-IR spectrum of the materials presented similar peaks to fresh material stretching from 1,500 to 420 cm^{-1}. The featured peaks of metal-N shifted slightly from 422.12 to 421.83 cm^{-1} (for catalyst) and 422.12 cm^{-1} (for adsorption), as seen in Figure 10a. Besides, the oscillation bonds of the imidazolate ring from 600 to 1,500 cm^{-1} still appeared with slight displacement compared to fresh material. In addition, the CuZn-ZIFs reused were examined for DBF residue on the material's surface, as described in the experiment above. Notably, the absence of DBF on the spectrum illustrated its desorption efficiency from the material during elution and recovery (Figure A7). Hence, the complete discard of DBF proved effective reusability for subsequent processing.

Furthermore, the XRD patterns observed that the CuZn-ZIFs reused had similar peaks, which were not significantly different compared with the fresh material. Obviously, the featured positions were at (011), (002), (112), (013), (222), (114), and (134), corresponding to these peaks' appearance in fresh material (Figure 10b). The aforementioned results demonstrated that the CuZn-ZIFs synthesized had excellent stability and reusability after multiple usages. Especially, CuZn-ZIFs not only possess both excellent adsorption and catalyst but also have a good

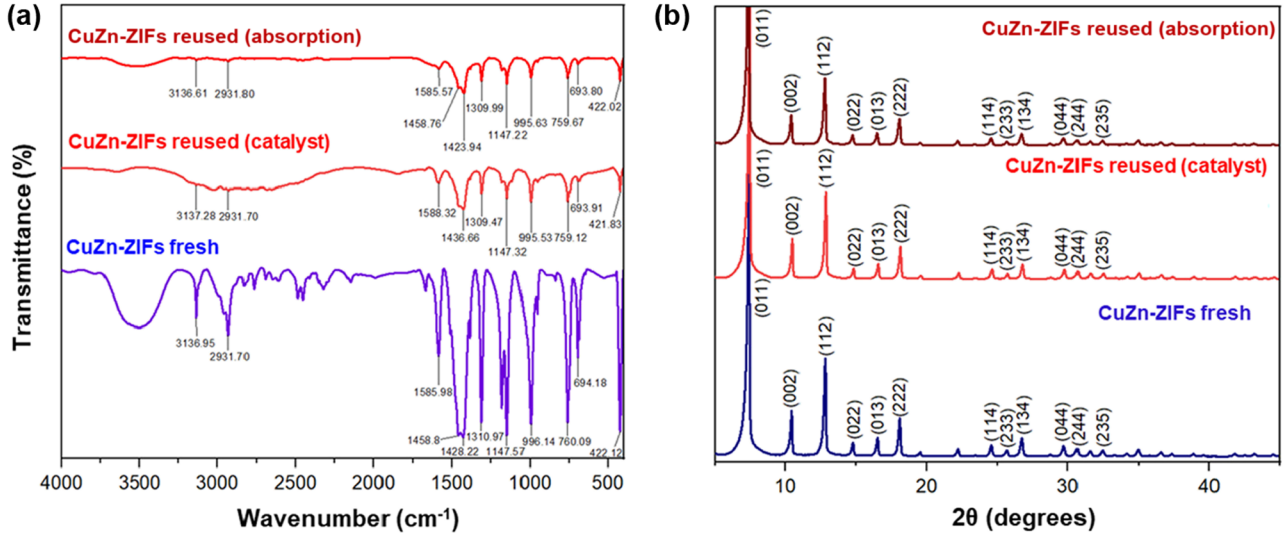

Figure 10: Structure analysis of CuZn-ZIFs reused after multiple cycles: (a) FT-IR pattern of CuZn-ZIFs reused and (b) PXRD pattern of CuZn-ZIFs reused.

regeneration ability without any appreciation loss over multiple cycles [57]. Conclusively, the CuZn-ZIFs are expected to be effective materials in DBF treatment, either directly or indirectly, and can be reused many times.

4 Conclusions

The successful synthesis of bimetallic CuZn-ZIFs was determined by characterization technique, i.e., PXRD, FT-IR, SEM, BET, EDX, and TGA to verify the changes within the framework structure and its composition. The optimal conditions for DBF treatment were confirmed with 10 mg CuZn-ZIFs, an initial DBF concentration of 30 ppm at room temperature within 40 min for adsorption, and 60 min for catalyst with the presence of 15 mM H_2O_2. Moreover, the reusability was confirmed due to the treatment's high efficiency of more than 80% for adsorption and 90% for catalyst after five recycle times since the first cycle, respectively. The mechanism of each process is based on its properties for adsorption and catalysis as a Fenton-like reaction in the previous report. Along with biological interventions such as microorganisms, for instance, bacteria degrade recalcitrant pollutants in soil, the material is a potential candidate for indirect/direct contaminants removal in water treatment and is economically viable and effective in reducing mortality by environmental pollutants. These results are important for further investigation into the effect of material structure on reaction performance, as well as the understanding of kinetic control strategies and practical application for contaminated water. Conclusively, this study provides the first evidence of the activity of bimetallic CuZn-ZIFs for degrading DBF as a member of UP-POPs via catalytic H_2O_2 decomposition.

Funding information: This study was funded by PEER Cycle 9 project, supported by USAID and NAS (US Government).

Author contributions: Thanh Q.C. Nguyen: writing – original draft, writing – review and editing, visualization, methodology; Huy B. Tran: visualization, methodology, formal analysis; Nghia K. Nguyen: project administration; Nhut M. Nguyen: writing – review and editing, visualization; and Giao H. Dang: writing – original draft, writing – review and editing, methodology, resources.

Conflict of interest: Authors state no conflict of interest.

References

[1] Chang H, Lin T, Whang L, Wu Y. Congener profiles of polychlorinated dibenzo-p-dioxins and polychlorinated dibenzofurans (PCDD/Fs) in sediment, water, and fish at a soil contamination site in Taiwan. J Environ Sci Health Part A. 2016;3:251–61. doi: 10.1080/10934529.2015.1094346.

[2] Custer TW, Custer CM, Gray BR. Polychlorinated biphenyls, dioxins, furans, and organochlorine pesticides in spotted sandpiper eggs from the upper Hudson River basin, New York. Ecotoxicology. 2010;19:391–404. doi: 10.1007/s10646-009-0425-z.

[3] Kirkok SK, Kibet JK, Kinyanjui TK, Okanga FI. A review of persistent organic pollutants: dioxins, furans, and their associated nitrogenated analogues. SN Appl Sci. 2020;2:1–20. doi: 10.1007/s42452-020-03551-y.

[4] Tuyet-hanh TT, Minh NH, Vu-anh L, Dunne M, Toms L, Tenkate T, et al. Environmental health risk assessment of dioxin in foods at the two most severe dioxin hot spots in Vietnam. Int J Hyg Environ Health. 2015;218:471–8. doi: 10.1016/j.ijheh.2015.03.014.

[5] Demond JLA, Franzblau A, Garabrant D, Jian X, Adriaens P, Chen Q, et al. Human exposure from dioxins in soil. Environ Sci Technol. 2012;46:1296–302. doi: 10.1021/es2022363.

[6] Terzaghi E, Vergani L, Mapelli F, Borin S, Raspa G, Zanardini E, et al. New data set of polychlorinated dibenzo-p-dioxin and dibenzofuran half-lives: natural attenuation and rhizoremediation using several common plant species in a weathered contaminated soil. Environ Sci Technol. 2020;54:10000–11. doi: 10.1021/acs.est.0c01857.

[7] Li X, Zhang S, Man R. Removal of polychlorinated dibenzo-p-dioxins and polychlorinated dibenzofurans by three coagulants in simulated coagulation processes for drinking water treatment. J Hazard Mater. 2009;162:180–5. doi: 10.1016/j.jhazmat.2008.05.030.

[8] Hadidi S, Shiri F. Chemosphere high selective gas-phase rearrangement reaction of TCDD induced by excess electron attachment: theoretical insight on the decomposition mechanism of one of the most toxic chemical known to science. Chemosphere. 2021;272:129617. doi: 10.1016/j.chemosphere.2021.129617.

[9] Kawamoto K, Weber R. Dioxin sources to the aquatic environment: re-assessing dioxins in industrial processes and possible emissions to the aquatic. Emerg Contam. 2021;7:52–62. doi: 10.1016/j.emcon.2021.01.002.

[10] Liu X, Wang J, Wang X, Zhu T. Chemosphere simultaneous removal of PCDD/Fs and NO_x from the flue gas of a municipal solid waste incinerator with a pilot plant. Chemosphere. 2015;133:90–6. doi: 10.1016/j.chemosphere.2015.04.009.

[11] Sun X, Sun T, Zhang Q, Wang W. Degradation mechanism of PCDDs initiated by OH radical in photo-Fenton oxidation technology: quantum chemistry and quantitative structure–activity relationship. Sci Total Environ. 2008;402:123–9. doi: 10.1016/j.scitotenv.2008.04.038.

[12] Buxton GV, Greenstock CL, Helman WP, Ross AB, Buxton GV, Greenstock CL, et al. Critical review of rate constants for reactions of hydrated electrons, hydrogen atoms and hydroxyl radicals (˙OH/˙O in aqueous solution. J Phys Chem Ref Data. 1988;17:513–886. doi: 10.1063/1.555805.

[13] Luong THV, Nguyen THT, Nguyen BV, Nguyen NK, Nguyen TQC, Dang GH. Efficient degradation of methyl orange and methylene blue in aqueous solution using a novel Fenton-like catalyst of CuCo-ZIFs. Green Process Synth. 2022;11:71–83. doi: 10.1515/gps-2022-0006.
[14] Wang N, Zheng T, Zhang G, Wang P. A review on Fenton-like processes for organic wastewater treatment. J Environ Chem Eng. 2016;4:762–87. doi: 10.1016/j.jece.2015.12.016.
[15] Bokare AD, Choi W. Review of iron-free Fenton-like systems for activating H_2O_2 in advanced oxidation processes. J Hazard Mater. 2014;275:121–35. doi: 10.1016/j.jhazmat.2014.04.054.
[16] Tang J, Salunkhe RR, Zhang H, Malgras V, Ahamad T, Alshehri SM, et al. Bimetallic metal-organic frameworks for controlled catalytic graphitization of nanoporous carbons. Sci Rep. 2016;6:3–4. doi: 10.1038/srep30295.
[17] Budi CS, Deka JR, Hsu WC, Saikia D, Chen KT, Kao HM, et al. Bimetallic Co/Zn zeolitic imidazolate framework ZIF-67 supported Cu nanoparticles: an excellent catalyst for reduction of synthetic dyes and nitroarenes. J Hazard Mater. 2020;407:124392. doi: 10.1016/j.jhazmat.2020.124392.
[18] Feng Y, Li Y, Xu M, Liu S, Yao J. Fast adsorption of methyl blue on zeolitic imidazolate framework-8 and its adsorption mechanism. RSC Adv. 2016;6:109608–12. doi: 10.1039/c6ra23870j.
[19] Chin M, Cisneros C, Araiza SM, Vargas KM, Ishihara KM, Tian F. Rhodamine B degradation by nanosized zeolitic imidazolate framework-8 (ZIF-8). RSC Adv. 2018;8:26987–97. doi: 10.1039/c8ra03459a.
[20] Nagarjun N, Dhakshinamoorthy A. A Cu-doped ZIF-8 metal organic framework as a heterogeneous solid catalyst for aerobic oxidation of benzylic hydrocarbons. N J Chem. 2019;43:18702–12. doi: 10.1039/c9nj03698a.
[21] Abdelhamid HN. Dye encapsulated hierarchical porous zeolitic imidazolate frameworks for carbon dioxide adsorption. J Environ Chem Eng. 2020;8:104008. doi: 10.1016/j.jece.2020.104008.
[22] Abdelhamid HN. Salts induced formation of hierarchical porous ZIF-8 and their applications for CO_2 sorption and hydrogen generation via $NaBH_4$ hydrolysis. Macromol Chem Phys. 2020;221:1–7. doi: 10.1002/macp.202000031.
[23] Abdelhamid HN. Hierarchical porous ZIF-8 for hydrogen production: via the hydrolysis of sodium borohydride. Dalton Trans. 2020;49:4416–24. doi: 10.1039/d0dt00145g.
[24] Hosseini H, Bolourian S, Yaghoubi Hamgini E, Ghanuni Mahababadi E. Optimization of heat- and ultrasound-assisted extraction of polyphenols from dried rosemary leaves using response surface methodology. J Food Process Preserv. 2018;42:1–15. doi: 10.1111/jfpp.13778.
[25] Xie W, Gao C, Li J. Sustainable biodiesel production from low-quantity oils utilizing $H_6PV_3MoW_8O_{40}$ supported on magnetic Fe_3O_4/ZIF-8 composites. Renew Energy. 2021;168:927–37. doi: 10.1016/j.renene.2020.12.129.
[26] Xie W, Wan F. Guanidine post-functionalized crystalline ZIF-90 frameworks as a promising recyclable catalyst for the production of biodiesel via soybean oil transesterification. Energy Convers Manag. 2019;198:111922. doi: 10.1016/j.enconman.2019.111922.
[27] Huang C, Liu R, Yang W, Li Y, Huang J, Zhu H. Enhanced catalytic activity of MnCo-MOF-74 for highly selective aerobic oxidation of substituted toluene. Inorg Chem Front View. 2018;5:1923–32. doi: 10.1039/C8QI00429C.
[28] Mitchell L, Williamson P, Ehrlichová B, Anderson AE, Seymour VR, Ashbrook SE, et al. Mixed-metal MIL-100 (Sc, M) (M = Al, Cr, Fe) for Lewis acid catalysis and tandem C–C bond formation and alcohol oxidation. Chem Eur J. 2014;20:17185–97. doi: 10.1002/chem.201404377.
[29] Abuzalat O, Tantawy H, Basuni M, Alkordi MH, Baraka A. Designing bimetallic zeolitic imidazolate frameworks (ZIFs) for aqueous catalysis: Co/Zn- ZIF-8 as a cyclic-durable catalyst for hydrogen peroxide oxidative decomposition of organic dyes in water. RSC Adv. 2022;12(10):6025–36. doi: 10.1039/d2ra00218c.
[30] Munoz M, De Pedro ZM, Pliego G, Casas JA, Rodriguez JJ. Chlorinated byproducts from the fenton-like oxidation of polychlorinated phenols. Ind Eng Chem Res. 2012;51:13092–9. doi: 10.1021/ie3013105.
[31] Poerschmann J, Trommler U, Górecki T, Kopinke FD. Formation of chlorinated biphenyls, diphenyl ethers and benzofurans as a result of Fenton-driven oxidation of 2-chlorophenol. Chemosphere. 2009;75:772–80. doi: 10.1016/j.chemosphere.2009.01.020.
[32] Lee JM, Kim JH, Chang YY, Chang YS. Steel dust catalysis for Fenton-like oxidation of polychlorinated dibenzo-p-dioxins. J Hazard Mater. 2009;163:222–30. doi: 10.1016/j.jhazmat.2008.06.081.
[33] Munoz M, de Pedro ZM, Casas JA, Rodriguez JJ. Assessment of the generation of chlorinated byproducts upon Fenton-like oxidation of chlorophenols at different conditions. J Hazard Mater. 2011;190:993–1000. doi: 10.1016/j.jhazmat.2011.04.038.
[34] Kim M, O'Keefe PW. Photodegradation of polychlorinated dibenzo-p-dioxins and dibenzofurans in aqueous solutions and in organic solvents. Chemosphere. 2000;41:793–800. doi: 10.1016/S0045-6535(99)00564-0.
[35] Katsumata H, Kaneco S, Suzuki T, Ohta K, Yobiko Y. Degradation of polychlorinated dibenzo-p-dioxins in aqueous solution by Fe(II)/H_2O_2/UV system. Chemosphere. 2006;63:592–9. doi: 10.1016/j.chemosphere.2005.08.015.
[36] Zhang J, Liu K. Enhanced adsorption of doxycycline hydrochloride (DCH) from water on zeolitic imidazolate framework-8 modified by Cu^{2+} (Cu–ZIF-8). Water Air Soil Pollut. 2020;231:91. doi: 10.1007/s11270-020-4455-8.
[37] Awadallah-F A, Hillman F, Al-Muhtaseb SA, Jeong HK. On the nanogate-opening pressures of copper-doped zeolitic imidazolate framework ZIF-8 for the adsorption of propane, propylene, isobutane, and n-butane. J Mater Sci. 2019;54:5513–27. doi: 10.1007/s10853-018-03249-y.
[38] Goyal S, Shaharun MS, Kait CF, Abdullah B. Effect of monometallic copper on zeolitic imidazolate framework-8 synthesized by hydrothermal method. J Phys Conf Ser. 2018;1123:012062. doi: 10.1088/1742-6596/1123/1/012062.
[39] Lu Y, Pan H, Lai J, Xia Y, Chen L, Liang R, et al. Bimetallic CoCu-ZIF material for efficient visible light photocatalytic fuel denitrification. RCS Adv. 2022;12:12702–09.
[40] Schejn A, Aboulaich A, Balan L, Falk V, Lalevée J, Medjahdi G, et al. Cu^{2+}-doped zeolitic imidazolate frameworks (ZIF-8): efficient and stable catalysts for cycloadditions and condensation reactions. Catal Sci Technol. 2015;3:10715–22. doi: 10.1039/b000000x.
[41] Parkash A. Copper doped zeolitic imidazole frameworks (ZIF-8): a new generation of single-atom catalyst for oxygen

reduction reaction in alkaline media. J Electrochem Soc. 2020;167(15):155504. doi: 10.1149/1945-7111/abaaa5.
[42] Nagarjun N, Arthy K, Dhakshinamoorthy A. Copper(II)-doped ZIF-8 as a reusable and size selective heterogeneous catalyst for the hydrogenation of alkenes using hydrazine hydrate. Eur J Inorg Chem. 2021;2021:2108–19. doi: 10.1002/ejic.202100126.
[43] Ahmad A, Iqbal N, Noor T, Hassan A, Khan UA, Wahab A, et al. Cu-doped zeolite imidazole framework (ZIF-8) for effective electrocatalytic CO_2 reduction. J CO_2 Util. 2021;48:101523. doi: 10.1016/j.jcou.2021.101523.
[44] Rueda-Márquez JJ, Levchuk I, Manzano M, Sillanpää M. Toxicity reduction of industrial and municipal wastewater by advanced oxidation processes (photo-Fenton, UVC/H_2O_2, electro-Fenton and galvanic Fenton): a review. Catalysts. 2020;10:612. doi: 10.3390/catal10060612.
[45] Vallejo M, Román MFS, Irabien A, Ortiz I. Comparative study of the destruction of polychlorinated dibenzo-p-dioxins and dibenzofurans during Fenton and electrochemical oxidation of landfill leachates. Chemosphere. 2013;90:132–8. doi: 10.1016/j.chemosphere.2012.08.018.
[46] Chanderia K, Kumar S, Sharma J, Ameta R, Punjabi PB. Degradation of sunset yellow FCF using copper loaded bentonite and H_2O_2 as photo-Fenton like reagent. Arab J Chem. 2017;10:S205–11. doi: 10.1016/j.arabjc.2012.07.023.
[47] Cai M, Hong Q, Sun J, Sundqvist K, Wiberg K, Chen K, et al. Concentrations, distribution and sources of polychlorinated dibenzo-p-dioxins and dibenzofurans and dioxin-like polychlorinated biphenyls in coastal sediments from Xiamen, China. Mar Chem. 2016;185:74–81. doi: 10.1016/j.marchem.2016.05.008.
[48] Mahmoodi NM, Ghezelbash M, Shabanian M, Aryanasab F, Saeb MR. Efficient removal of cationic dyes from colored wastewaters by dithiocarbamate-functionalized graphene oxide nanosheets: from synthesis to detailed kinetics studies. J Taiwan Inst Chem Eng. 2017;81:1–8. doi: 10.1016/j.jtice.2017.10.011.
[49] Kim H, Masaki H, Matsumura T, Kamei T. Removal efficiency and homologue patterns of dioxins in drinking water treatment. Water Res. 2002;36:4861–9.
[50] Gao S, Hou J, Cheetham AK, Liang K, Chen V, Gao S, et al. Improving the acidic stability of zeolitic imidazolate frameworks by biofunctional molecules. Chem. 2019;5:1597–608. doi: 10.1016/j.chempr.2019.03.025.
[51] Parnklang T, Lamlua B, Gatemala H. Shape transformation of silver nanospheres to silver nanoplates induced by redox reaction of hydrogen peroxide. Mater Chem Phys. 2015;153:10–7. doi: 10.1016/j.matchemphys.2014.12.044.
[52] Pham AN, Xing G, Miller CJ, Waite TD. Fenton-like copper redox chemistry revisited: hydrogen peroxide and superoxide mediation of copper-catalyzed oxidant production. J Catal. 2013;301:54–64. doi: 10.1016/j.jcat.2013.01.025.
[53] Burg A, Shusterman I, Kornweitz H, Meyerstein D. Three H_2O_2 molecules are involved in the "Fenton-like" reaction between $Co(H2O)_6^{2+}$ and H_2O_2. Dalton Trans. 2014;43:9111–5. doi: 10.1039/c4dt00401a.
[54] Kuśmierek K, Kiciński W, Norek M, Polański M, Budner B. Oxidative and adsorptive removal of chlorophenols over Fe-, N- and S-multi-doped carbon xerogels. J Environ Chem Eng. 2021;9:105568. doi: 10.1016/j.jece.2021.105568.
[55] Dang GH, Le TTA, Ta AK, Ho TNT, Pham TV, Doan TVH, et al. Removal of Congo red and malachite green from aqueous solution using heterogeneous Ag/ZnCo-ZIF catalyst in the presence of hydrogen peroxide. Green Process Synth. 2020;9:567–77. doi: 10.1515/gps-2020-0060.
[56] Chen L, Wang HF, Li C, Xu Q. Bimetallic metal-organic frameworks and their derivatives. Chem Sci. 2020;11:5369–5403. doi: 10.1039/d0sc01432j.
[57] Chen J, Gu A, Djam E, Liu Y, Wang P, Mao P, et al. Cu-Zn bimetal ZIFs derived nanowhisker zero-valent copper decorated ZnO nanocomposites induced oxygen activation for high-efficiency iodide elimination. J Hazard Mater. 2021;416:126097. doi: 10.1016/j.jhazmat.2021.126097.
[58] Park H, Reddy DA, Kim Y, Ma R, Choi J, Kim TK, et al. Zeolitic imidazolate framework-67 (ZIF-67) rhombic dodecahedrons as full-spectrum light harvesting photocatalyst for environmental remediation. Solid State Sci. 2016;62:82–9.

Appendix

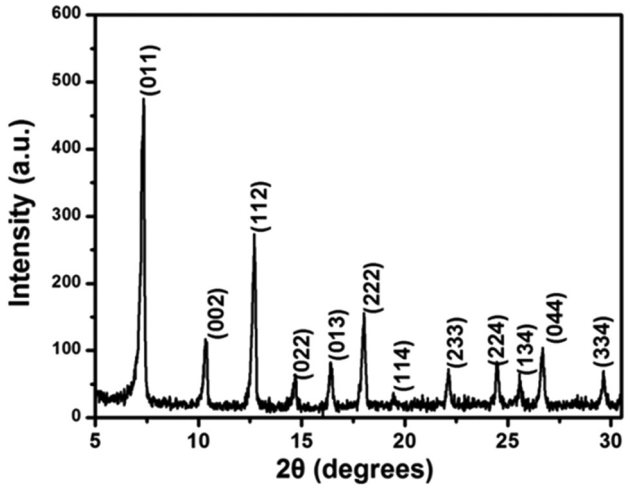

Figure A1: PXRD pattern of ZIF-67 [58].

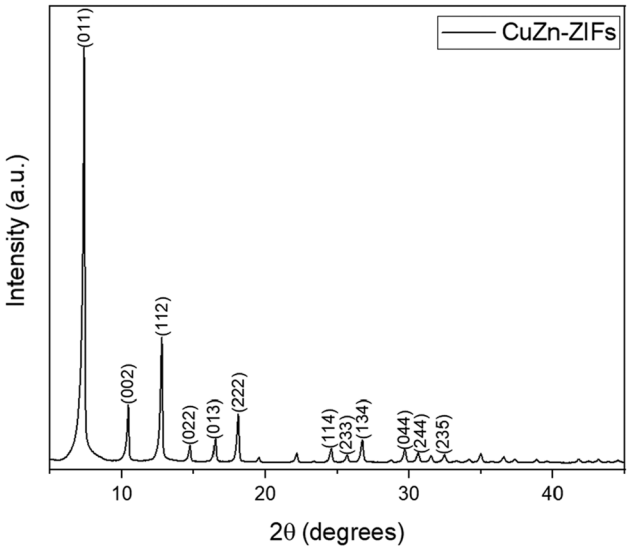

Figure A3: PXRD pattern of CuZn-ZIFs.

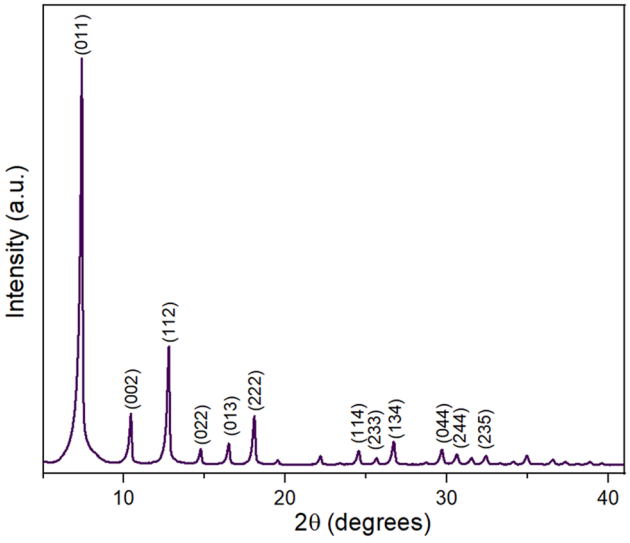

Figure A2: PXRD pattern of ZIF-8.

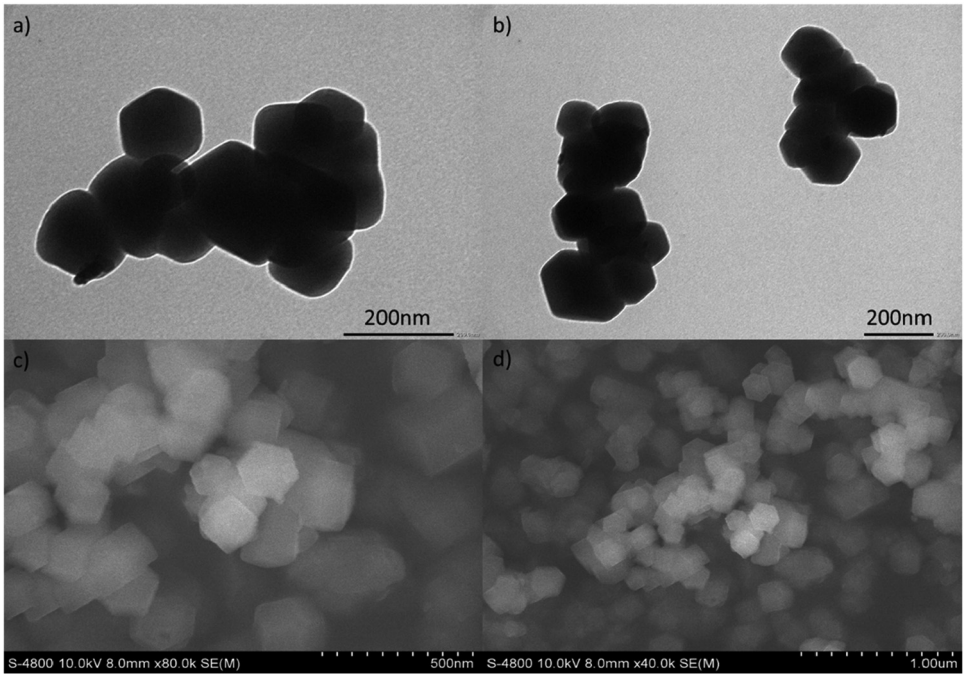

Figure A4: TEM images of CuZn-ZIFs (a, b: 20,000×) and SEM images of CuZn-ZIFs (c: 80,000×, d: 40,000×).

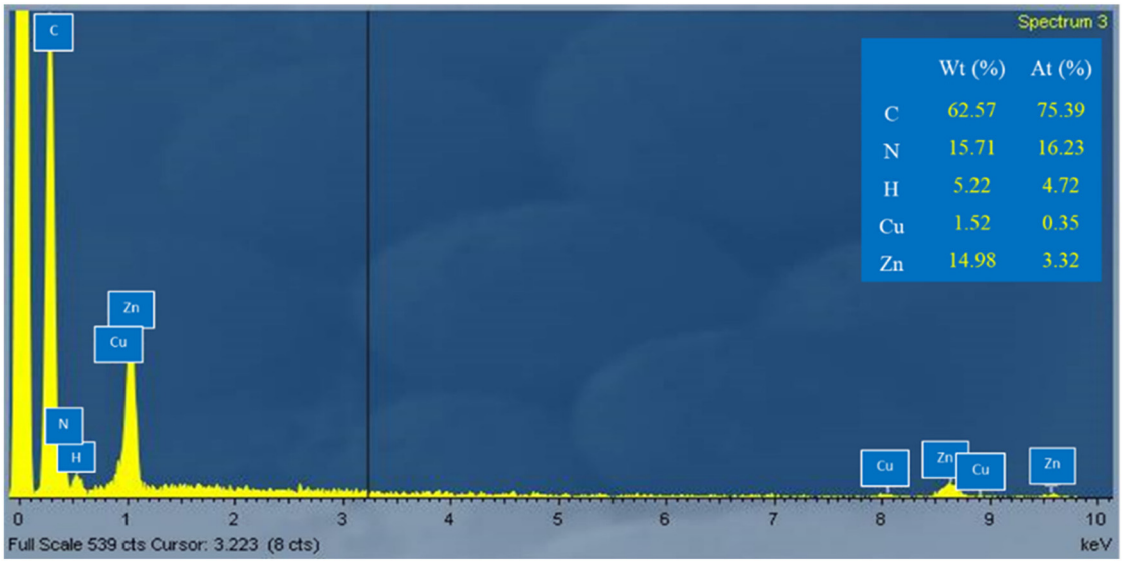

Figure A5: EDX spectra of CuZn-ZIFs.

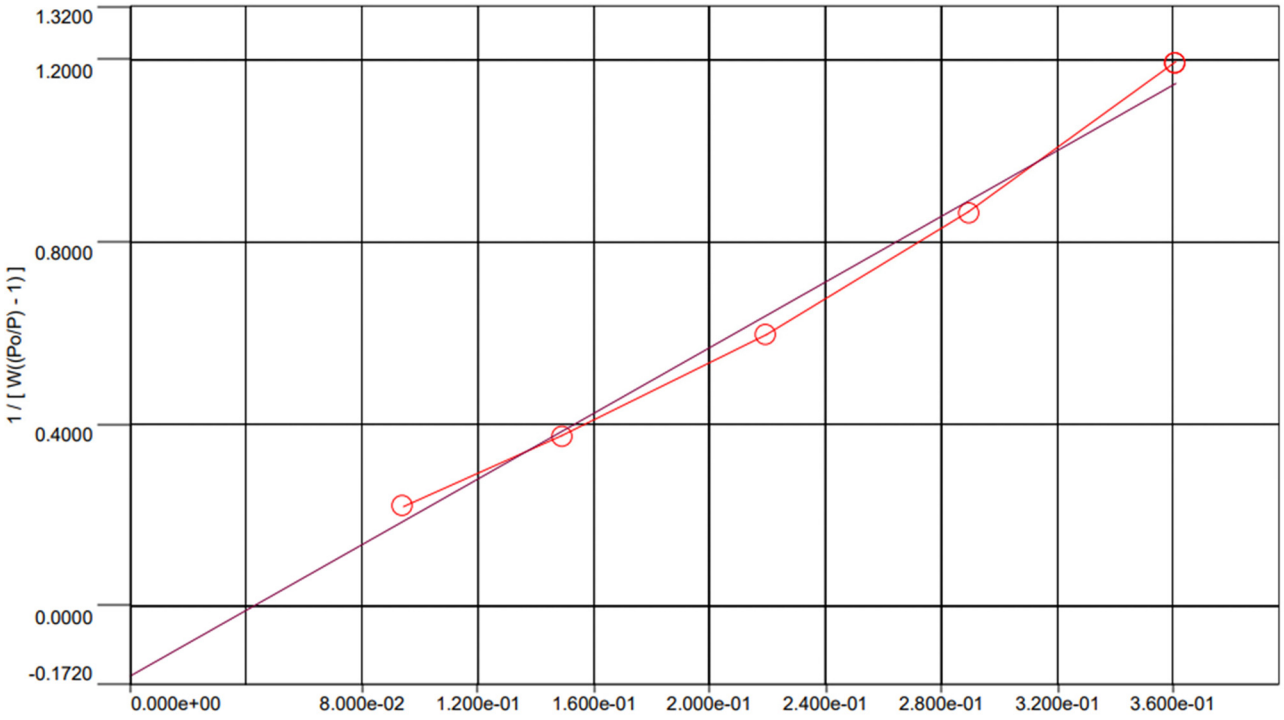

Multi-Point BET Data

Relative Pressure [P/Po]	Volume @ STP [cc/g]	1 / [W((Po/P) - 1)]	Relative Pressure [P/Po]	Volume @ STP [cc/g]	1 / [W((Po/P) - 1)]
9.38370e-02	373.4540	2.2186e-01	2.89795e-01	377.3717	8.6514e-01
1.48912e-01	375.3125	3.7300e-01	3.60722e-01	378.1944	1.1938e+00
2.19424e-01	376.4778	5.9742e-01			

BET summary

Slope =	3.623
Intercept =	-1.561e-01
Correlation coefficient, r =	0.995078
C constant=	-22.214
Surface Area =	1004.411 m²/g

Figure A6: Nitrogen adsorption–desorption isotherm of CuZn-ZIFs.

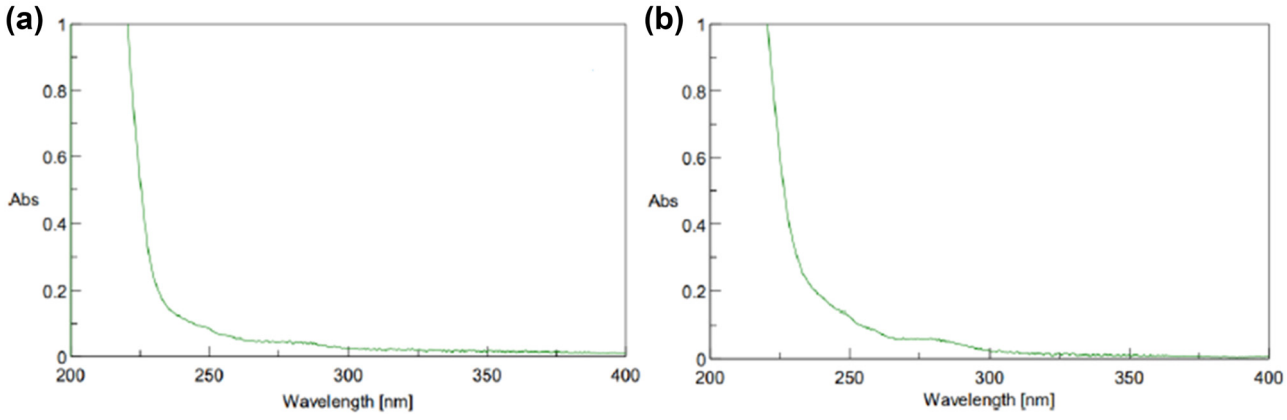

Figure A7: (a) UV-Vis spectrum of DBF residue after washing in adsorption process and (b) UV-Vis spectrum of DBF residue after adding HCl in adsorption process.

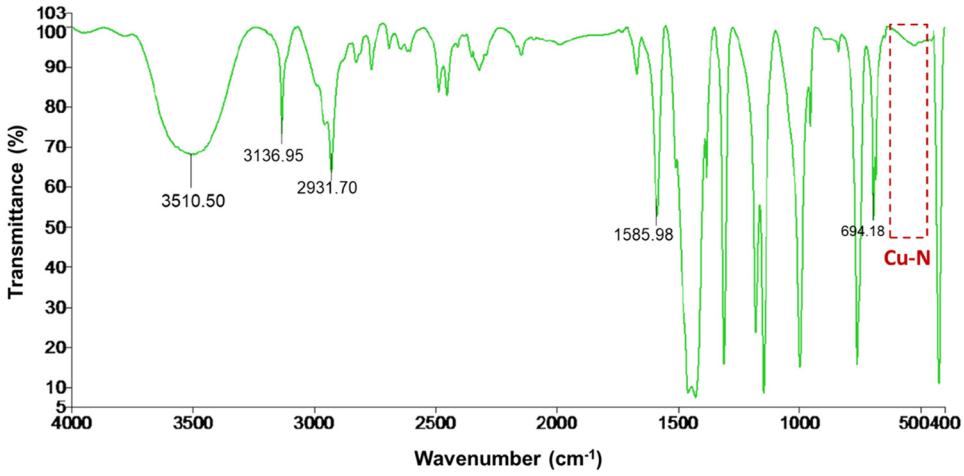

Figure A8: FT-IR pattern of CuZn-ZIFs.